# USING SENTINEL-2 IMAGERY TO TRACK CHANGES PRODUCED BY *XYLELLA FASTIDIOSA* IN OLIVE TREES

*Alberto Hornero[a,b*], Rocio Hernández-Clemente[a], Pieter S.A. Beck[c], Juan A. Navas-Cortés[b], Pablo J. Zarco-Tejada[c]*

[a] Department of Geography, Swansea University, SA2 8PP Swansea, UK
[b] Instituto de Agricultura Sostenible (IAS), Consejo Superior de Investigaciones Científicas (CSIC), Alameda del Obispo S/N, 14004, Córdoba, Spain
[c] European Commission, Joint Research Centre (JRC), Directorate D – Sustainable Resources - Bio-Economy Unit, Via E. Fermi 2749 – TP 261, 26a/043, I-21027 Ispra, VA, Italy
[*]Corresponding author. A. Hornero <alberto.hornero@csic.es>

## ABSTRACT

This paper attempts to provide an understanding of the potential application of Sentinel-2 imagery for the monitoring and detection of disease symptoms caused by *Xylella fastidiosa* (*Xf*) in olive trees. A time series data of 188 Sentinel-2a images collected over the last two years was used to analyse the temporal trends in areas with *Xf* infected olive trees in Puglia, Southern Italy. The robustness of different physiological and structural hyperspectral indices was evaluated as an early indicator of *Xf* symptoms. Three validation sites for Sentinel-2a products were hence established over olive orchards in the *Xf*-infected zone in two different years (2016 and 2017) and overflown with a hyperspectral sensor to acquire high spatial resolution images (50 cm). Disease incidence and severity levels were recorded for more than 3300 olive trees in 18 orchards. Results demonstrate the capability of temporal Sentinel-2a was able to detect and discriminate between high and medium *Xf* incidence, reaching the maximum differences during the summer season. Among all the vegetation indices evaluated from Sentinel-2 imagery, OSAVI showed superior performance for detecting *Xf* incidence trends and OSAVI$_{1510}$ for detecting changes in *Xf* severity levels.

*Index Terms*— Sentinel-2, hyperspectral, *Xylella fastidiosa*, olive-tree, die-back, temporal trend

## 1. INTRODUCTION

*Xylella fastidiosa (Xf)*, a plant pathogenic bacteria that lives in plants' water-conducting system is causing severe damage in multiple plant species and compromising the production of key crops all over the world [1]. The first *Xf* outbreak in Europe was detected in Apulia (south-eastern Italy) in olive orchards [2], [3]. Severe infections cause withering and desiccation of the canopy and can result in dieback, stunting an eventual death of the tree [4]. Detecting and monitoring spatial changes and disease outbreaks is critical to design effective surveillance strategies [5]. In addition, it is critical to accurately discriminate different stages of the development of the disease in order to map its spread [6], [7] and to monitor the damage over large areas. Spatial and temporal data provided by satellite images open new possibilities for developing monitoring methods. Sentinel-2 data combines temporal, spatial and spectral resolution in an unprecedented way. Nonetheless, also at the spatial resolution of Sentinel-2 data, soil and backgrounds effects are expected to play a confounding role in the monitoring of sparse and well-spaced orchard canopies.

Hence, there is a clear need to investigate the possibility of using Sentinel-2 data, and vegetation indices derived from them, to detect the incidence and spread of *Xf* in olive-dominated landscapes. Here, we present new field experiments and multi-temporal data analysis to test the capability of physiological and structural hyperspectral and Sentinel-2 indices as indicators of the incidence and severity of *Xf*-outbreaks in olive orchards.

## 2. MATERIAL AND METHODS

### 2.1. Data collection

The study area is an olive growth area in the region of Apulia, Italy. We assessed both disease incidence and severity of *Xf*-symptoms between June 2016 and July 2017 by visually inspecting 3300 individual olive trees in 18 orchards; the evaluated disease severity was rated on a 0-4 scale depending on canopy desiccation and the proportion of the crown affected; from 0 indicating the absence of visible symptoms to 4 indicating most branches are dead. All olive orchards evaluated were located within the Xf infected zone in Puglia region. The visible symptoms detected such as chlorosis and defoliation were related to the disease, as demonstrated by laboratory qPCR analysis.

The Multispectral Instrument (MSI) on board Sentinel-2a acquires imagery with ten-day revisit times under constant viewing conditions which results in 4-6 days at mid-latitudes due to its swath width from contiguous orbits. The MSI measurements provide radiance in 13 spectral bands from VNIR to SWIR, with images at 12-bit per channel and with a spectral resolution of 10 m (CWL at 496.6, 560.0, 664.5, and 835.1 nm with an FWHM of 98, 45, 38 and 145 nm, respectively), 20 m (CWL at 703.9, 740.2, 782.5, 864.8, 1613.7 and 2202.4 nm with an FWHM of 19, 18, 28, 33, 143 and 242 nm, respectively) and 60 m (CWL at 443.9, 945.0 and 1373.5 nm with an FWHM of 27, 26 and 75 nm, respectively).

We obtained the Sentinel-2a images of the study area from July 2015 to August 2017. They were atmospherically corrected from Level-1C (TOA reflectance) to generate Level-2A with Sen2Cor (version 2.3.1). Cloud-free Sentinel-2a imagery was filtered and processed considering the Scene Classification from Level-2a and then a time-series was generated for different vegetation indices. Due to atmospheric variability and in order to fill the gaps in the seasonal data, a Local Polynomial Regression Fitting [8] was applied to smooth out noise in the time-series for each index.

Airborne campaigns were conducted on 28 June 2016, and 3 July 2017, using a hyperspectral imager – Micro-Hyperspec VNIR model (Headwall Photonics Inc., Fitchburg, MA, USA) – on board a Cessna aircraft. Near-infrared and visible spectral regions (400-885 nm) were covered by operating the sensor with 260 bands and a radiometric resolution of 12 bits; at 1.865 nm central wavelength (CWL) interval, yielding 6.4 nm full width at half maximum (FWHM) with a 25-micron slit. Flight details and sensor configuration can be found in [9]. Image correction and data pre-processing are described in detail in [10], [11].

## 2.2. Data analysis

For this study, we calculated several spectral vegetation indices (VI) mainly related to canopy structure and pigment composition. In particular, we tested i) conventional and corrected ratio and normalized differential indices derived from the near-infrared and red bands such as NDVI, MSR, GNDVI, and RDVI, ii) conventional soil-adjusted indices such as SAVI, Optimized Soil Adjusted Vegetation Index (OSAVI) and Modified Soil Adjusted Vegetation Index (MSAVI), and corrected versions using SWIR bands such as OSAVI$_{1510}$, iii) conventional and corrected chlorophyll vegetation indices such as CI, NDI, MTCI, PSSRa, S2REP, IRECI and iii) narrow-band chlorophyll indices formulated to minimize their sensitivity to structural effect based on the Chlorophyll Absorption in Reflectance Index (CARI) and its transformations into TCARI & MCARI normalized by OSAVI in the form TCARI/OSAVI and MCARI$_{1510}$ using

SWIR bands. A detailed description of this selection of vegetation indices and their formulation can be found in [10].

After the spectral data from Sentinel-2 were validated with the hyperspectral imager data, the temporal Sentinel-2 evolution within two consecutive years was used to test if VI trends differed between areas dominated by trees with high and medium *Xf* incidence.

We used Pearson correlation analysis and *p*-values to determine the significance and strength of the relationship between the temporal VI dataset and the two different in-situ measures of *Xf* outbreaks: severity and incidence.

## 3. RESULTS

NDVI and OSAVI products across sensors (Sentinel-2a and the hyperspectral imager) showed very similar patterns (Fig. 1) at the study sites for 2016 with $r^2=0.73$, $p<0.001$ for NDVI and $r^2=0.68$, $p<0.001$ for OSAVI, and for 2017 with $r^2=0.71$, $p<0.001$ for NDVI and $r^2=0.74$, $p<0.001$ for OSAVI. The temporal consistency between the two data sets lends credibility to the temporal patterns in the Sentinel-2a VIs.
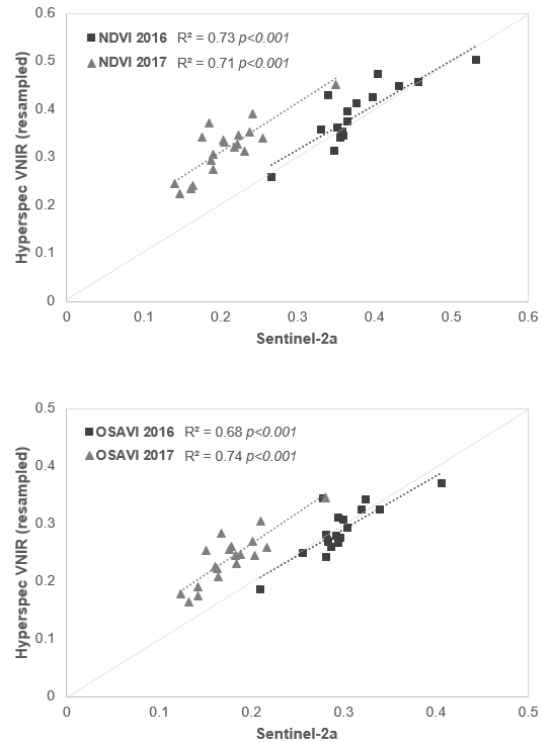




Fig.1. Cross-validation of the Sentinel-2a dataset and high-resolution hyperspectral images: relationship for NDVI between both sensors with images collected in 2016 (*n=18*) and 2017 (*n=19*).

The analysis of the temporal evolution of Sentinel-2a NDVI data revealed significant differences in the trends of medium and high *Xf* incidence over the last two years. The greatest

differences were reached during the summer season. Figure 2 compares the average of the plots showing the highest recorded level of damage (high incidence increase) and those with a medium level of damage (medium incidence increase).
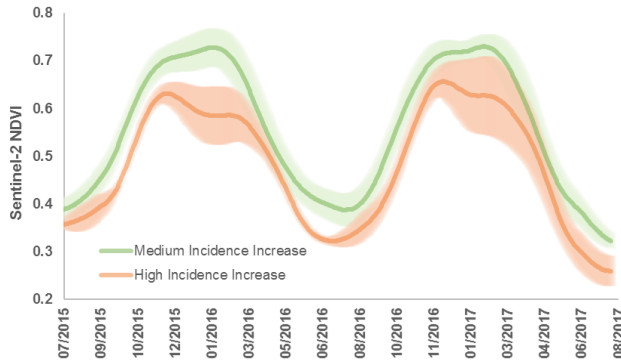


Fig.2. Monthly mean NDVI trend for plots with medium and high *Xf* incidence increase. Shaded areas represent the monthly standard deviation.

The strength of the correlation between changes in several spectral indices and the *Xf* outbreak measures is shown in Fig. 3. Significant correlations were found between the incidence increase and the vegetation indices OSAVI ($r=0.91$, $p<0.001$), RDVI ($r=0.87$, $p<0.001$), NDVI ($r=0.86$, $p<0.001$), MSR ($r=0.82$, $p<0.001$), NDI ($r=0.81$, $p<0.001$) and TCARI ($r=0.78$, $p<0.01$). In contrast, only OSAVI$_{1510}$ and MCARI were significantly correlated to the severity increase, yielding correlation coefficients of ($r=0.65$, $p<0.001$) and ($r=0.47$, $p<0.001$) respectively.



Fig. 3. Relationship between severity and incidence increase and all Sentinel-2a vegetation indices selected for this study. Correlation coefficient ranges from -1 to 1, in red and green, respectively. Cross symbols indicate non-significant relationships ($p$-values$>0.01$).

## 4. CONCLUSIONS

This study shows the sensitivity of Sentinel-2 imagery to canopy alterations produced by progressive *Xf* infection in olive orchards. Our results indicate OSAVI and OSAVI$_{1510}$ can be used to robustly monitoring orchard-level changes in *Xf*-incidence and outbreak severity, respectively. They, therefore, suggest that Sentinel-2 data can provide useful spatio-temporal indicators to track and map the damage caused by *Xf* infections across large areas.

## 6. REFERENCES

[1] R. P. P. Almeida and L. Nunney, "How Do Plant Diseases Caused by Xylella fastidiosa Emerge?," *Plant Dis.*, vol. 99, no. 11, pp. 1457–1467, Oct. 2015.

[2] A. Abbott, "Italy rebuked for failure to prevent olive-tree tragedy," *Nat. News*, vol. 546, no. 7657, p. 193, Jun. 2017.

[3] A. Abbott, "Gridlock over Italy's olive tree deaths starts to ease," *Nat. News*, vol. 533, no. 7603, p. 299, May 2016.

[4] EFSA-PLH, "Treatment solutions to cure Xylella fastidiosa diseased plants," *EFSA J.*, vol. 14, no. 4, p. n/a-n/a, Apr. 2016.

[5] K. Usha and B. Singh, "Potential applications of remote sensing in horticulture—A review," *Sci. Hortic.*, vol. 153, no. Supplement C, pp. 71–83, Apr. 2013.

[6] M. Saponari *et al.*, "Isolation and pathogenicity of Xylella fastidiosa associated to the olive quick decline syndrome in southern Italy," *Sci. Rep.*, vol. 7, no. 1, p. 17723, Dec. 2017.

[7] C. R. Girelli *et al.*, "Xylella fastidiosa and olive quick decline syndrome (CoDiRO) in Salento (southern Italy): a chemometric 1H NMR-based preliminary study on Ogliarola salentina and Cellina di Nardò cultivars," *Chem. Biol. Technol. Agric.*, vol. 4, no. 1, p. 25, Dec. 2017.

[8] W. S. Cleveland, E. Grosse, and W. M. Shyu, "Local regression models," *Stat. Models S*, vol. 2, pp. 309–376, 1992.

[9] P. J. Zarco-Tejada, A. Morales, L. Testi, and F. J. Villalobos, "Spatio-temporal patterns of chlorophyll fluorescence and physiological and structural indices acquired from hyperspectral imagery as compared with carbon fluxes measured with eddy covariance," *Remote Sens. Environ.*, vol. 133, pp. 102–115, Jun. 2013.

[10] P. J. Zarco-Tejada, M. V. González-Dugo, and E. Fereres, "Seasonal stability of chlorophyll fluorescence quantified from airborne hyperspectral imagery as an indicator of net photosynthesis in the context of precision agriculture," *Remote Sens. Environ.*, vol. 179, pp. 89–103, Jun. 2016.

[11] R. Hernández-Clemente, R. M. Navarro-Cerrillo, and P. J. Zarco-Tejada, "Carotenoid content estimation in a heterogeneous conifer forest using narrow-band indices and PROSPECT + DART simulations," *Remote Sens. Environ.*, vol. 127, pp. 298–315, Dec. 2012.